Editors' Suggestion | Featured in Physics

Polar Fluctuations Lead to Extensile Nematic Behavior in Confluent Tissues

Andrew Killeen,[1] Thibault Bertrand,[2,*] and Chiu Fan Lee[1,†]
[1]Department of Bioengineering, Imperial College London, South Kensington Campus, London SW7 2AZ, United Kingdom
[2]Department of Mathematics, Imperial College London, South Kensington Campus, London SW7 2AZ, United Kingdom

(Received 8 July 2021; revised 10 November 2021; accepted 6 January 2022; published 15 February 2022)

How can a collection of motile cells, each generating contractile nematic stresses in isolation, become an extensile nematic at the tissue level? Understanding this seemingly contradictory experimental observation, which occurs irrespective of whether the tissue is in the liquid or solid states, is not only crucial to our understanding of diverse biological processes, but is also of fundamental interest to soft matter and many-body physics. Here, we resolve this cellular to tissue level disconnect in the small fluctuation regime by using analytical theories based on hydrodynamic descriptions of confluent tissues, in both liquid and solid states. Specifically, we show that a collection of microscopic constituents with no inherently nematic extensile forces can exhibit active extensile nematic behavior when subject to polar fluctuating forces. We further support our findings by performing cell level simulations of minimal models of confluent tissues.

DOI: 10.1103/PhysRevLett.128.078001

A key aim in many-body physics is to connect microscopic dynamics to macroscopic, system-level behavior, and a fundamental difficulty in this task is that emergent behavior at the macroscopic level can be very different from what one would expect from the microscopic picture [1]. A case in point is planar confluent epithelial tissue dynamics—while a single motile epithelial cell on a substrate can exhibit polar dynamics [2,3] and generate contractile nematic stress when its cell shape is elongated [4], a confluent monolayer of these cells can instead act like an extensile nematic [5]. Throughout this Letter, the nematic tensor field refers to the *direction of cell shape elongation*. Intriguingly, this disconnect between the cellular and tissue dynamics is robust and present no matter whether the tissue is in the liquid or solid states. The cause of this discrepancy remains poorly understood in both cases. Resolving the seemingly contradictory behavior at the single-cell versus the tissue level is not only important to active matter physics, but is also crucial to a number of fundamental biological processes. In eukaryotes, extensile nematic defects have been shown to mediate cell extrusions in epithelial monolayers [5] and control the collective dynamics of neural progenitor cell cultures [6]. In collectives of microorganisms, they are responsible for initiating layer formation in *Myxococcus xanthus* colonies [7], mediating the morphologies of growing *E. coli* colonies [8], controlling morphogenesis in *Hydra* [9], and increasing collective migration velocities of *Pseudomonas aeruginosa* [10].

Naturally, active nematic liquid crystal theories have become an emerging paradigm for characterizing the dynamics of these biological systems [6,11–15]. Active nematic systems are typically characterized by elongated constituents possessing apolar motility [16], and it is well established that activity can induce local nematic order [17–19]. Therefore, it is not surprising that previous studies focused on the emergence of active nematic defects in these systems. For example, in *Myxococcus xanthus* colonies, individual bacteria are rod shaped and display periodic reversals of velocity direction prior to fruiting body formation [20]. Other biological constituents that exhibit collective nematic behavior usually possess at least one of these two features, such as the spindle shape of fibroblasts or the active forces involved in cell division being inherently dipolar [12,21,22]. However, epithelial cells are not rod shaped and display polar dynamics [2,3], calling into question whether active nematic liquid crystal theories capture the fundamental physics of epithelial monolayers.

Recent studies have tried to resolve the discrepancy between cell-level and tissue-level dynamics in epithelial tissues [23,24], with one study notably linking polar activity to extensile active nematic behavior [24]. However, both these studies directly incorporate *ad hoc* extensile nematic terms into the equations of motion (EOM), either in the deterministic part [23] or in the fluctuation part [24]. Doing so begs the following question: Are we missing key microscopic, cell-level ingredients to justify these terms? In this Letter, we refute this need by showing, analytically and by simulation, that polar fluctuations (due to cell-substrate interactions) generically lead to extensile nematic behavior in a confluent tissue, in *both* liquid and solid states. Our conclusion applies universally in the small fluctuation limits when active contractile nematic stresses are absent in the system. When contractile stresses are switched on at the cellular level (due to cellular contractility and cell-cell interactions [25]), the nematic nature of the confluent tissue can be either extensile or contractile depending on, e.g., the relative strengths of the

polar fluctuations and the fluctuations of the active nematic stresses.

In the following, we will first analyze a generic set of linearized EOM describing the velocity and nematic fields (characterizing the direction of the cell shape elongation) of confluent cell tissues, and then illustrate our findings by simulating confluent tissues in the liquid and solid states using an active vertex model [26,27].

Analytical argument.—We first consider a generic model of 2D confluent cell tissue in the liquid state. Consistent with previous studies, we will treat confluent tissues with polar fluctuations as an incompressible active fluid on a frictional substrate [28–31], in which the polar fluctuations originate from cell-substrate interactions; we ignore thermal fluctuations as they are negligible in cellular and tissue dynamics. To capture the coarse-grained cell shape anisotropy, we use the nematic tensor field $\mathbf{Q} = S(2\hat{\mathbf{n}}\hat{\mathbf{n}} - 1)$, where S is the scalar nematic order parameter and $\hat{\mathbf{n}}$ is the local coarse-grained unit director that corresponds to the elongated direction of the cell [32].

Motivated by *in vitro* experimental studies on epithelial tissues, we focus on the regime without long-range order in the velocity field $\mathbf{v}$ [31] or quasi-long-range order in the nematic field $\mathbf{Q}$ [36–38], and away from the order-disorder critical region [39]. While we do not expect the system to develop any hydrodynamic soft modes in this regime, it is still of interest to use the hydrodynamic equations to study the system at length scales beyond the microscopic (cellular) length scale. In the small fluctuations regime, the magnitudes of both $\mathbf{v}$ and $\mathbf{Q}$ are small and thus the linearized EOM are expected to apply universally; these are of the form

$$\partial_t \mathbf{v} = \mu \nabla^2 \mathbf{v} - \boldsymbol{\nabla} P - \Gamma \mathbf{v} + \alpha \boldsymbol{\nabla} \cdot \mathbf{Q} + \boldsymbol{\xi}, \tag{1a}$$

$$\partial_t \mathbf{Q} = \lambda [\boldsymbol{\nabla}\mathbf{v} + (\boldsymbol{\nabla}\mathbf{v})^{\mathsf{T}}] + D\nabla^2 \mathbf{Q} - \eta \mathbf{Q}, \tag{1b}$$

where the polar fluctuations $\boldsymbol{\xi}$, originating from cell-substrate interactions such as transient lamellipodia activity [3,25], are represented by a Gaussian white noise with

$$\begin{aligned} \langle \xi_i(t, \mathbf{r}) \rangle &= 0, \\ \langle \xi_i(t, \mathbf{r}) \xi_j(t', \mathbf{r}') \rangle &= 2\Delta \delta_{ij} \delta(t - t') \delta^2(\mathbf{r} - \mathbf{r}'). \end{aligned} \tag{2}$$

Indeed, while the cells' polar fluctuations typically display some persistency, in the hydrodynamic limit (i.e., at long enough time and length scales), this persistency is irrelevant and these fluctuations can be described as δ-correlated noise terms as in Eq. (2). This is akin to systems of self-propelled particles being described by the Toner-Tu equations in the hydrodynamic limit [28,29,40]. The "pressure" P in Eq. (1a) acts as a Lagrange multiplier here to enforce the incompressibility condition $\boldsymbol{\nabla} \cdot \mathbf{v} = 0$. Further, we have included an active nematic term, $\alpha \boldsymbol{\nabla} \cdot \mathbf{Q}$, in the EOM of $\mathbf{v}$ (1a), and the diffusivity parameter D is proportional to the nematic stiffness (in the one-elastic constant approximation) [24,41].

We will focus first on the case of passive nematics [$\alpha = 0$ in Eq. (1a)]. In the highly damped limits (large Γ and η), we can set both temporal derivatives in Eq. (1) to zero. In this regime, applying a divergence to Eq. (1b) leads to

$$(\eta - D\nabla^2) \boldsymbol{\nabla} \cdot \mathbf{Q} = \lambda \nabla^2 \mathbf{v}. \tag{3}$$

In Fourier transformed space, we have

$$\mathrm{i} k_j \tilde{Q}_{ij} = -\frac{\lambda k^2 \tilde{v}_i}{\eta + Dk^2}, \tag{4}$$

where we have used Einstein's summation convention.

To ascertain the extensile or contractile nature of the nematic field, we calculate the equal-time, equal-position correlation $\langle \mathbf{v} \cdot (\boldsymbol{\nabla} \cdot \mathbf{Q}) \rangle$. The motivation behind doing so is that an active nematic material is usually characterized as extensile or contractile by the sign of the coefficient α in front of the active nematic term $\alpha \boldsymbol{\nabla} \cdot \mathbf{Q}$ when present. Focusing on Eq. (1a) and ignoring all spatial and temporal variations, it is clear that the sign of α is the same as that of the correlation $\langle \mathbf{v} \cdot (\boldsymbol{\nabla} \cdot \mathbf{Q}) \rangle$. Therefore, even if $\alpha = 0$, calculating such a correlation enables us to ascertain effectively the extensile or contractile nature of the nematic field under the system's dynamics.

The correlation is given by [32]

$$\langle \mathbf{v} \cdot (\boldsymbol{\nabla} \cdot \mathbf{Q}) \rangle = -2\lambda\Delta \int \frac{d^2\mathbf{k}}{(2\pi)^2} \frac{k^2}{(Dk^2 + \eta)(\mu k^2 + \Gamma)^2}. \tag{5}$$

The integral above is always positive (in fact, it equals $[(D\Gamma + \mu\eta\{\log[\mu\eta/(D\Gamma)] - 1\})/(4\pi\mu(D\Gamma - \mu\eta)^2)]$ when integrating over all wavelength $\mathbf{k}$). Therefore, the correlation between $\mathbf{v}$ and $\boldsymbol{\nabla} \cdot \mathbf{Q}$ depends only on the sign of λ. Specifically, the nematic field is statistically extensile if $\lambda > 0$, and contractile if $\lambda < 0$. In the case of confluent cell tissues, it is clear that a positive velocity gradient will cause a cell to stretch in the direction of that gradient. Hence, λ is positive and thus statistically, the velocity field is negatively correlated with the divergence of the nematic field. In other words, *a polar fluctuation in confluent cell tissues will generically lead to the appearance of active extensile nematics*. In Ref. [32], we show that this conclusion can in fact be generalized to compressible tissues in the fluid state.

However, active contractile nematic behavior in cell tissues has also been observed experimentally, e.g., in fibroblasts cells [13,42]. In the context of active nematics, one can recover this behavior by setting $\alpha > 0$ in Eq. (1a). Additionally, since the nematic field $\mathbf{Q}$ can now generate active stresses, fluctuations in the EOM of $\mathbf{Q}$ are also generically present. Specifically, one needs to include a Gaussian noise term $\boldsymbol{\Omega}$ on the r.h.s. of Eq. (1b), with statistics given by

$$\langle \Omega_{ij}(t,\mathbf{r})\rangle = 0, \tag{6a}$$

$$\langle \Omega_{ij}(t,\mathbf{r})\Omega_{kl}(t',\mathbf{r}')\rangle = 2\Delta_Q \delta(t-t')\delta^2(\mathbf{r}-\mathbf{r}')\epsilon_{ijkl}, \tag{6b}$$

where, for symmetry reasons,

$$\epsilon_{ijkl} = \frac{1}{2}(\delta_{ik}\delta_{jl} + \delta_{il}\delta_{jk} - \delta_{ij}\delta_{kl}). \tag{7}$$

Repeating the analysis with the terms $\alpha\boldsymbol{\nabla}\cdot\mathbf{Q}$ and $\boldsymbol{\Omega}$ added to Eqs. (1a) and (1b), respectively, we find that the correlation $\langle \mathbf{v}\cdot(\boldsymbol{\nabla}\cdot\mathbf{Q})\rangle$ now takes the following form

$$\langle \mathbf{v}\cdot(\boldsymbol{\nabla}\cdot\mathbf{Q})\rangle = \int \frac{d^2\mathbf{k}}{(2\pi)^2(Dk^2+\eta)}\left\{-2\lambda\Delta k^2 G(k)^2 + \alpha\Delta_Q k^2\left[\frac{G(k)}{Dk^2+\eta} - \frac{\alpha\lambda k^2 G(k)^2}{(Dk^2+\eta)^2}\right]\right\}, \tag{8}$$

where $G(k) = \{\mu k^2 + \Gamma + [\lambda\alpha k^2/(Dk^2+\eta)]\}^{-1}$ (see Ref. [32] for details). Note that in the case where $\alpha = 0$, one naturally recovers the expression in Eq. (5). For positive α and λ, the terms in the square bracket in the integral (8) are always positive overall [32]. Hence, the system can transition from exhibiting extensile nematic behavior to contractile nematic behavior when the terms in the square bracket dominate over the first one. In particular, this transition happens when the dimensionless ratio $\alpha\Delta_Q/\lambda\Delta$ is much greater than 1 [32].

We note here that our results so far are qualitatively and quantitatively different from a recent work on the same topic [24] in the following ways: (i) both the active stress term ($\propto \alpha$) and fluctuations in $\mathbf{Q}$ are crucial for the extensile-contractile transition in our work [since it is the product $\alpha\Delta_Q$ that appears in the correlation (8)], (ii) we do not assume that the nematic field influences the polar fluctuations, and (iii) nonlinear advective coupling is not needed in our treatment. Indeed, while nonlinear effects may be crucial in the high fluctuation limits, it remains unclear how to gauge the importance of a particular nonlinear term in relations to (many) other nonlinear terms that are intrinsically present in the EOM. In the present theory, nonlinear effects are not relevant since we focus exclusively on the small fluctuation limits.

Having established the expected extensile nematic behavior in confluent tissues in the liquid state, we now repeat the analysis in the solid state, again in the highly damped limits. Here, the relevant hydrodynamic variables are the displacement field $\mathbf{u}$ from the stress-free configuration, as well as the velocity field $\mathbf{v}$ and the passive nematic field $\mathbf{Q}$. The linear EOM in this case read [43]

$$\Gamma\mathbf{v} = A\nabla^2\mathbf{u} + B\boldsymbol{\nabla}(\boldsymbol{\nabla}\cdot\mathbf{u}) + \boldsymbol{\xi}, \tag{9a}$$

$$\eta\mathbf{Q} = C[\boldsymbol{\nabla}\mathbf{u} + (\boldsymbol{\nabla}\mathbf{u})^{\mathsf{T}}] + \lambda[\boldsymbol{\nabla}\mathbf{v} + (\boldsymbol{\nabla}\mathbf{v})^{\mathsf{T}}] + D\nabla^2\mathbf{Q}, \tag{9b}$$

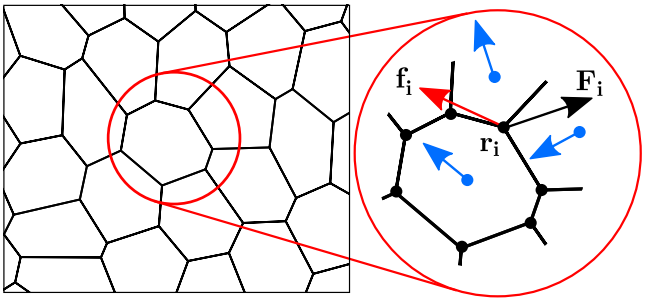

FIG. 1. Schematic of the active vertex model (AVM). The degrees of freedom are the cell vertices (black dots). Each vertex experiences two types of forces, an active force from cellular self-propulsion, $\mathbf{f}_i$ (red arrow), which is the mean self-propulsive force from the 3 cells that neighbor each vertex (blue arrows), and the mechanical response of the tissue to this driving, $\mathbf{F}_i$ (black arrow).

where the constants A and B are the shear modulus and bulk modulus of the material, respectively, both of which are positive [43], and $\boldsymbol{\xi}$ is a polar fluctuation term again given by Eq. (2). The coupling constant C between the strain and nematic fields leads to the development of strain anisotropy either parallel ($C > 0$) or perpendicular ($C < 0$) to $\mathbf{Q}$ [44]. We expect it to be positive for the same reason—outlined previously—that we expect λ to be positive, although the sign does not affect our result. We can now analyze Eq. (9) following a similar procedure [32] as in the liquid case to conclude that *polar fluctuations in the solid state generically lead to extensile nematic dynamics in cell shapes*.

Simulation results.—To validate our analytical results, we perform simulations on a cell-based model of confluent tissues in both liquid and solid states [45]. Vertex based models represent an important class of models which have successfully reproduced several experimental observations [26,46–48]. Therefore, we use the active vertex model (AVM) to explore the dynamics of the tissue in both solid and liquid states. As in previous studies, we focus on the dynamics of $+1/2$ defects to determine the extensile or contractile nature of the nematic field [49].

We implement an AVM following Ref. [27]. We represent the monolayer as a tiling of polygons; the cell vertices are the degrees of freedom in this model, and each cell is endowed with a self-propulsive motile force (Fig. 1). In addition to self-propulsion, vertices move in response to mechanical interactions stemming from the following effective tissue energy function

$$E = \sum_{a=1}^{N} K_A(A_a - A_0)^2 + K_P(P_a - P_0)^2, \tag{10}$$

where N is the number of cells, K_A and K_P are the area and perimeter moduli, A_a and P_a are the area and perimeter of cell a, and A_0 and P_0 are the target area and perimeter common to all cells. The first term in Eq. (10) is quadratic

in the cell areas and encodes a combination of cell volume incompressibility and the monolayer's resistance to height fluctuations. The second term in the energy function is quadratic in the perimeter of the cells and encodes a competition between the contractility of the actomyosin cortex and cell membrane tension from cell-cell adhesion and cortical tension. The interaction force on vertex m is then $\mathbf{F}_m = -\nabla_m E$.

The AVM undergoes a rigidity transition that is controlled by the target shape index $p_0 = P_0/\sqrt{A_0}$ [50]. In passive systems, this transition occurs at $p_0 = p_0^* \approx 3.81$, although this decreases with increasing active motility [26]. Above this critical value of p_0^* there are no energy barriers to cell rearrangements and the cell layer enters a liquidlike phase, rearranging via T1 transitions. We thus choose values of p_0 and active mobility strength to ensure $p_0 < p_0^*$ for our solid simulation and $p_0 > p_0^*$ for our liquid simulation.

To model cell motility, each cell is endowed with a self-propulsion force of constant magnitude, f_0. This self-propulsion force acts along a polarity vector, $\hat{\mathbf{n}}_a = (\cos\theta_a, \sin\theta_a)$, where θ_a is an angle measured from the x axis. The resultant self-propulsion force on each vertex is the average self-propulsion force of the three cells that neighbor vertex m, $\mathbf{f}_m = (f_0/3)\sum_{a\in\mathcal{N}(m)} \hat{\mathbf{n}}_a$, where $\mathcal{N}(m)$ denotes the list of cells that share vertex m. Assuming overdamped dynamics, the EOM for each vertex, with position $\mathbf{r}_m$, is

$$\frac{d\mathbf{r}_m}{dt} = \frac{1}{\zeta}(\mathbf{F}_m + \mathbf{f}_m), \tag{11}$$

where ζ is the damping coefficient. Finally, the polarity vector of each cell also undergoes rotational diffusion according to

$$\frac{d\theta_a}{dt} = \sqrt{2D_r}\xi_a(t), \tag{12}$$

where D_r is the rotational diffusion coefficient and $\xi_a(t)$ is a white noise process with zero mean and unit variance. In both liquid and solid states, we present results for monolayers of 400 cells on a periodic domain with uniformly distributed initial polarities. The AVM only explicitly includes polar active forces, meaning it is comparable to our analytical model without the inclusion of active contractility. Therefore, extensile behavior is expected universally.

Following Refs. [5] and [42], we compute the instantaneous cell orientation field and implement a defect detection algorithm [32]. Despite its simplicity, we observe that the AVM, in both solid and liquid states, displays $\pm 1/2$ defects generated randomly within the tissue in a similar manner to those observed in epithelial layers *in vitro* [5] [Figs. 2(a)–2(d), left]. Upon computing mean properties of the tissue around these defects, we observe velocity fields

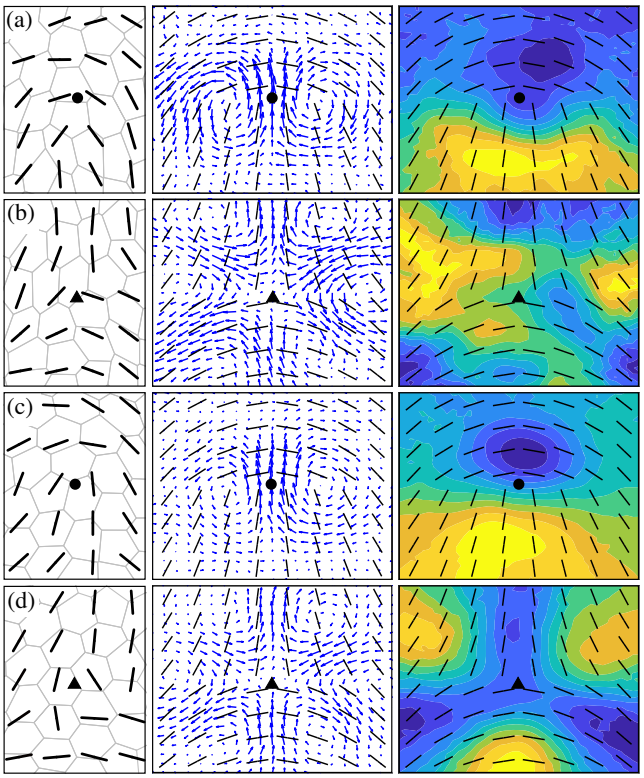

FIG. 2. Simulation results of confluent tissues in their liquid [(a) and (b)] and solid [(c) and (d)] states. Nematic configurations, dynamics, and passive stress fields around detected $+1/2$ defects in the (a) liquid state and (c) solid state, and those of detected $-1/2$ defects in the (b) liquid state and (d) solid state. In each case, we show representative defects (left), mean velocity fields around defects (middle), and heat maps of mean isotropic passive stress $(\sigma_{xx} + \sigma_{yy})/2$ due to cell-cell interactions around defects (right). Heat maps have been normalized such that blue represents maximum compression and yellow maximum tension. We use $A_0 = 1$, $K_A = 1$, $K_P = 1$, $f_0 = 0.5$, and $D_r = 1$. In the liquid state we use $P_0 = 3.7$ and in the solid state $P_0 = 3.4$. See the Supplemental Material for details of simulation procedures and defect detection methodology [32].

indicative of extensile active nematic behavior, with the +1/2 defect moving in a tail to head direction [Figs. 2(a) and 2(c), middle] [49]. We also show the mean passive isotropic stress due to cell-cell interactions in Figs. 2(a)–2(d), (right). We note that the only type of topological defects consistently observed were defects with half-integer charges. Further, the extensile behavior is apparent over a range of stiffnesses and activities, and collective contractile behavior was never seen over the parameter ranges explored. Additionally, we numerically determine the correlation calculated in our analytical model [32]. We find that, for both solid and liquid states, the numerical correlation is always negative overall. Overall, our simulation results fully support our analytical findings.

Discussion and outlook.—We demonstrate analytically that planar confluent tissues with polar fluctuations lead

generically to extensile nematic behavior with regards to cell shape orientation. In contrast to previous studies, our analysis does not require the addition of *ad hoc* extensile nematic terms [8,23,24]. Further, our analytical treatment applies universally in the small fluctuation regime and thus elucidates how extensile behavior can emerge even though contractile nematic stresses are prevalent at the cellular scale. We confirm all our findings by simulating models of confluent tissues in both liquid and solid states.

We note that a recent joint experimental and theoretical work investigating the switch from contractile cells to extensile tissues concluded that the extensile behavior of epithelial tissues may come from strong intercellular interactions mediated by cadherins [42]. Our result here is consistent with their findings if stronger intercellular interactions lead to a reduction in the fluctuations or strength of the active nematic contractility due to the increased rigidity at the cellular level. Additionally, a recent study has found that cadherin-mediated cell-cell contacts support the formation of cryptic lamellipodia [51], meaning stronger intercellular interactions could also facilitate stronger polar traction forces.

Finally, since our main motivation comes from experiments, we focus here exclusively on confluent tissues, however, we expect our theory to apply equally to many-body systems of deformable particles or elongated particles. Indeed, we argue that our results could explain the previously unresolved extensile motion of +1/2 defects seen in 2D layers of rod-shaped molecules on a vibrating substrate [52]. Other interesting future directions include the investigation of the dynamics of cell shapes in the ordered regimes [31,53] and close to the order-disorder critical regime [39].

We thank Benoit Ladoux and Lakshmi Balasubramaniam for helpful advice and discussion regarding calculation of the director field and defect detection, and acknowledge the High Throughput Computing service provided by Imperial College Research Computing Service. A. K. was supported by the EPSRC Centre for Doctoral Training in Fluid Dynamics Across Scales (Grant No. EP/L016230/1).

*t.bertrand@imperial.ac.uk
†c.lee@imperial.ac.uk

[1] P. W. Anderson, More is different, Science **177**, 393 (1972).
[2] F. J. Segerer, F. Thüroff, A. Piera Alberola, E. Frey, and J. O. Rädler, Emergence and Persistence of Collective Cell Migration on Small Circular Micropatterns, Phys. Rev. Lett. **114**, 228102 (2015).
[3] S. Jain, V. M. Cachoux, G. H. Narayana, S. de Beco, J. D'Alessandro, V. Cellerin, T. Chen, M. L. Heuzé, P. Marcq, R. M. Mège, A. J. Kabla, C. T. Lim, and B. Ladoux, The role of single-cell mechanical behaviour and polarity in driving collective cell migration, Nat. Phys. **16**, 802 (2020).
[4] W. Pomp, K. Schakenraad, H. E. Balcloğlu, H. Van Hoorn, E. H. J. Danen, R. M. H. Merks, T. Schmidt, and L. Giomi, Cytoskeletal Anisotropy Controls Geometry and Forces of Adherent Cells, Phys. Rev. Lett. **121**, 178101 (2018).
[5] T. B. Saw, A. Doostmohammadi, V. Nier, L. Kocgozlu, S. Thampi, Y. Toyama, P. Marcq, C. T. Lim, J. M. Yeomans, and B. Ladoux, Topological defects in epithelia govern cell death and extrusion, Nature (London) **544**, 212 (2017).
[6] K. Kawaguchi, R. Kageyama, and M. Sano, Topological defects control collective dynamics in neural progenitor cell cultures, Nature (London) **545**, 327 (2017).
[7] K. Copenhagen, R. Alert, N. S. Wingreen, and J. W. Shaevitz, Topological defects promote layer formation in myxococcus xanthus colonies, Nat. Phys. **17**, 211 (2021).
[8] A. Doostmohammadi, S. P. Thampi, and J. M. Yeomans, Defect-Mediated Morphologies in Growing Cell Colonies, Phys. Rev. Lett. **117**, 048102 (2016).
[9] Y. Maroudas-Sacks, L. Garion, L. Shani-Zerbib, A. Livshits, E. Braun, and K. Keren, Topological defects in the nematic order of actin fibres as organization centres of hydra morphogenesis, Nat. Phys. **17**, 251 (2021).
[10] O. J. Meacock, A. Doostmohammadi, K. R. Foster, J. M. Yeomans, and W. M. Durham, Bacteria solve the problem of crowding by moving slowly, Nat. Phys. **17**, 205 (2021).
[11] D. Volfson, S. Cookson, J. Hasty, and L. S. Tsimring, Biomechanical ordering of dense cell populations, Proc. Natl. Acad. Sci. U.S.A. **105**, 15346 (2008).
[12] G. Duclos, S. Garcia, H. G. Yevick, and P. Silberzan, Perfect nematic order in confined monolayers of spindle-shaped cells, Soft Matter **10**, 2346 (2014).
[13] G. Duclos, C. Erlenkämper, J. F. Joanny, and P. Silberzan, Topological defects in confined populations of spindle-shaped cells, Nat. Phys. **13**, 58 (2017).
[14] G. Duclos, C. Blanch-Mercader, V. Yashunsky, G. Salbreux, J. F. Joanny, J. Prost, and P. Silberzan, Spontaneous shear flow in confined cellular nematics, Nat. Phys. **14**, 728 (2018).
[15] N. D. Bade, R. D. Kamien, R. K. Assoian, and K. J. Stebe, Edges impose planar alignment in nematic monolayers by directing cell elongation and enhancing migration, Soft Matter **14**, 6867 (2018).
[16] T. B. Saw, W. Xi, B. Ladoux, and C. T. Lim, Biological tissues as active nematic liquid crystals, Adv. Mater. **30**, 1802579 (2018).
[17] A. Baskaran and M. C. Marchetti, Hydrodynamics of self-propelled hard rods, Phys. Rev. E **77**, 011920 (2008).
[18] S. P. Thampi, A. Doostmohammadi, R. Golestanian, and J. M. Yeomans, Intrinsic free energy in active nematics, Europhys. Lett. **112**, 28004 (2015).
[19] S. Santhosh, M. R. Nejad, A. Doostmohammadi, J. M. Yeomans, and S. P. Thampi, Activity induced nematic order in isotropic liquid crystals, J. Stat. Phys. **180**, 699 (2020).
[20] S. Thutupalli, M. Sun, F. Bunyak, K. Palaniappan, and J. W. Shaevitz, Directional reversals enable Myxococcus xanthus cells to produce collective one-dimensional streams during fruiting-body formation, J. R. Soc. Interface **12**, 20150049 (2015).
[21] A. Doostmohammadi, S. P. Thampi, T. B. Saw, C. T. Lim, B. Ladoux, and J. M. Yeomans, Celebrating Soft Matter's 10th Anniversary: Cell division: A source of active stress in cellular monolayers, Soft Matter **11**, 7328 (2015).

[22] Z. You, D. J. G. Pearce, A. Sengupta, and L. Giomi, Geometry and Mechanics of Microdomains in Growing Bacterial Colonies, Phys. Rev. X **8**, 031065 (2018).
[23] R. Mueller, J. M. Yeomans, and A. Doostmohammadi, Emergence of Active Nematic Behavior in Monolayers of Isotropic Cells, Phys. Rev. Lett. **122**, 048004 (2019).
[24] F. Vafa, M. J. Bowick, B. I. Shraiman, and M. C. Marchetti, Fluctuations can induce local nematic order and extensile stress in monolayers of motile cells, Soft Matter **17**, 3068 (2021).
[25] T. Svitkina, The actin cytoskeleton and actin-based motility, Cold Spring Harbor Perspect. Biol. **10**, a018267 (2018).
[26] D. Bi, X. Yang, M. C. Marchetti, and M. L. Manning, Motility-Driven Glass and Jamming Transitions in Biological Tissues, Phys. Rev. X **6**, 021011 (2016).
[27] D. M. Sussman, cellGPU: Massively parallel simulations of dynamic vertex models, Comput. Phys. Commun. **219**, 400 (2017).
[28] J. Toner and Y. Tu, Long-Range Order in a Two-Dimensional Dynamical *XY* Model: How Birds Fly Together, Phys. Rev. Lett. **75**, 4326 (1995).
[29] J. Toner and Y. Tu, Flocks, herds, and schools: A quantitative theory of flocking, Phys. Rev. E **58**, 4828 (1998).
[30] H. H. Wensink, J. Dunkel, S. Heidenreich, K. Drescher, R. E. Goldstein, H. Löwen, and J. M. Yeomans, Meso-scale turbulence in living fluids, Proc. Natl. Acad. Sci. U.S.A. **109**, 14308 (2012).
[31] L. Chen, C. F. Lee, and J. Toner, Mapping two-dimensional polar active fluids to two-dimensional soap and one-dimensional sandblasting, Nat. Commun. **7**, 12215 (2016).
[32] See Supplemental Material at http://link.aps.org/supplemental/10.1103/PhysRevLett.128.078001 for further analytical and simulation details, which includes Refs. [33–35].
[33] D. Huterer and T. Vachaspati, Distribution of singularities in the cosmic microwave background polarization, Phys. Rev. D **72**, 043004 (2005).
[34] A. J. Vromans and L. Giomi, Orientational properties of nematic disclinations, Soft Matter **12**, 6490 (2016).
[35] X. Yang, D. Bi, M. Czajkowski, M. Merkel, M. L. Manning, and M. C. Marchetti, Correlating cell shape and cellular stress in motile confluent tissues, Proc. Natl. Acad. Sci. U.S.A. **114**, 12663 (2017).
[36] S. Mishra, A. Simha, and S. Ramaswamy, A dynamic renormalization group study of active nematics, J. Stat. Mech. (2010) P02003.
[37] S. Shankar, S. Ramaswamy, and M. C. Marchetti, Low-noise phase of a two-dimensional active nematic system, Phys. Rev. E **97**, 012707 (2018).
[38] P. Sartori and C. F. Lee, Scaling behaviour of non-equilibrium planar N -atic spin systems under weak fluctuations, New J. Phys. **21**, 073064 (2019).
[39] L. Chen, J. Toner, and C. F. Lee, Critical phenomenon of the order-disorder transition in incompressible active fluids, New J. Phys. **17**, 042002 (2015).
[40] M. C. Marchetti, J. F. Joanny, S. Ramaswamy, T. B. Liverpool, J. Prost, M. Rao, and R. A. Simha, Hydrodynamics of soft active matter, Rev. Mod. Phys. **85**, 1143 (2013).
[41] S. Ramaswamy, A. Simha, and J. Toner, Active nematics on a substrate: Giant number fluctuations and long-time tails, Europhys. Lett. **62**, 196 (2003).
[42] L. Balasubramaniam, A. Doostmohammadi, T. B. Saw, G. H. N. S. Narayana, R. Mueller, T. Dang, M. Thomas, S. Gupta, S. Sonam, A. S. Yap, Y. Toyama, R.-M. Mège, J. M. Yeomans, and B. Ladoux, Investigating the nature of active forces in tissues reveals how contractile cells can form extensile monolayers, Nat. Mater. **20**, 1156 (2021).
[43] L. D. Landau, E. M. Lifshitz, A. M. Kosevich, J. B. Sykes, L. P. Pitaevskii, and W. H. Reid, *Theory of Elasticity: Volume 7*, Course of Theoretical Physics (Elsevier Science, New York, 1986).
[44] A. Maitra and S. Ramaswamy, Oriented Active Solids, Phys. Rev. Lett. **123**, 238001 (2019).
[45] M. R. Shaebani, A. Wysocki, R. G. Winkler, G. Gompper, and H. Rieger, Computational models for active matter, Nat. Rev. Phys. **2**, 181 (2020).
[46] D. L. Barton, S. Henkes, C. J. Weijer, and R. Sknepnek, Active vertex model for cell-resolution description of epithelial tissue mechanics, PLoS Comput. Biol. **13**, e1005569 (2017).
[47] V. Petrolli, M. Le Goff, M. Tadrous, K. Martens, C. Allier, O. Mandula, L. Hervé, S. Henkes, R. Sknepnek, T. Boudou, G. Cappello, and M. Balland, Confinement-Induced Transition between Wavelike Collective Cell Migration Modes, Phys. Rev. Lett. **122**, 168101 (2019).
[48] S. Henkes, K. Kostanjevec, J. M. Collinson, R. Sknepnek, and E. Bertin, Dense active matter model of motion patterns in confluent cell monolayers, Nat. Commun. **11**, 1405 (2020).
[49] L. Giomi, M. J. Bowick, P. Mishra, R. Sknepnek, and M. Cristina Marchetti, Defect dynamics in active nematics, Phil. Trans. R. Soc. A **372**, 20130365 (2014).
[50] D. Bi, J. H. Lopez, J. M. Schwarz, and M. L. Manning, A density-independent rigidity transition in biological tissues, Nat. Phys. **11**, 1074 (2015).
[51] M. Ozawa, S. Hiver, T. Yamamoto, T. Shibata, S. Upadhyayula, Y. Mimori-Kiyosue, and M. Takeichi, Adherens junction regulates cryptic lamellipodia formation for epithelial cell migration, J. Cell Biol. **219**, e202006196 (2020).
[52] V. Narayan, S. Ramaswamy, N. Menon, T. Caspt, and T. Caspt, Long-lived giant number fluctuations in a swarming granular nematic, Science **317**, 105 (2007),.
[53] F. Giavazzi, M. Paoluzzi, M. Macchi, D. Bi, G. Scita, M. L. Manning, R. Cerbino, and M. C. Marchetti, Flocking transitions in confluent tissues, Soft Matter **14**, 3471 (2018).